Available online at www.sciencedirect.com
SCIENCE DIRECT
Icarus 178 (2005) 253–263
ICARUS
www.elsevier.com/locate/icarus

Growth of planetesimals by impacts at ~25 m/s

Gerhard Wurm *, Georgi Paraskov, Oliver Krauss

Institute for Planetology, Wilhelm-Klemm-Str. 10, D-48149 Münster, Germany

Received 3 February 2005; revised 4 April 2005

Available online 31 May 2005

Abstract

We study central collisions between millimeter-sized dust projectiles and centimeter-sized dust targets in impact experiments. Target and projectile are dust aggregates consisting of micrometer-sized SiO_2 particles. Collision velocities range up to 25 m/s. The general outcome of a collision strongly depends on the impact velocity. For collisions below 13 m/s rebound and a small degree of fragmentation occur. However, at higher collision velocities up to 25 m/s approximately 50% of the mass of the projectile rigidly sticks to the target after the collision. Thus, net growth of a body is possible in high speed collisions. This supports the idea that planetesimal formation via collisional growth is a viable mechanism at higher impact velocities. Within our set of parameters the experiments even suggest that higher impact velocities might be preferable for growth in collisions between dusty bodies. For the highest impact velocities most of the ejecta is within small dust aggregates about 500 µm in size. In detail the size distribution of ejected dust aggregates is flat for very small particles smaller than 500 µm and follows a power law for larger ejected dust aggregates with a power of -5.6 ± 0.2. There is a sharp upper cut-off at about 1 mm in size with only a few particles being slightly larger. The ejection angle is smaller than 3° with respect to the target surface. These fast ejecta move with $40 \pm 10\%$ of the impact velocity.

Keywords: Planetesimals; Planetary formation; Collisional physics; Solar nebula; Experimental techniques

1. Introduction

It is common belief that (at least) terrestrial planets form through collisions of smaller bodies in protoplanetary disks (Beckwith et al., 2000; Wetherill and Stewart, 1989; Kokubo and Ida, 2002). Usually a size of the order of 1 km is considered as the initial size of the bodies which are called planetesimals. A question answered less unanimous is how planetesimals themselves form. A few decades ago it seemed that gravitational instability of a dense dust disk would easily yield objects of the right size (Goldreich and Ward, 1973). The model turned out to have serious problems though since shear induced turbulence would not allow a density high enough to be reached (Weidenschilling et al., 1989). There is ongoing work with respect to this model (e.g., Yamoto and Sekiya, 2004). Youdin and Shu (2002) suggested that under certain conditions instability is possible but only after several million years. While this might be just in time before disks on average dissolve, gravitational conditions might not be reachable in time if conditions are less ideal than assumed (Garaud and Lin, 2004; Haisch et al., 2001). Another more recent idea is that eddies which might develop in protoplanetary disks might collect small bodies in their center which might then grow to planetesimals or larger (Klahr and Bodenheimer, 2003).

A simpler idea for planetesimal formation is based on the mechanism of sticking collisions of smaller bodies which begins with (sub)-micrometers dust particles and eventually leads to the growth of planetesimals (Weidenschilling and Cuzzi, 1993; Weidenschilling, 1997; Beckwith et al., 2000). Over the last decade a number of experiments have been carried out to verify this model. They show that growth of centimeter-sized bodies in general can be understood in terms of a binary collision model (Wurm and Blum, 1998; Blum and Wurm, 2000; Blum et al., 2000). This was also

* Corresponding author. Fax: +49 251 8336301.
E-mail address: gwurm@uni-muenster.de (G. Wurm).

0019-1035/$ – see front matter
doi:10.1016/j.icarus.2005.04.002

found to be in agreement with theoretical studies of collisions of dust aggregates (Dominik and Tielens, 1997; Kempf et al., 1999). During this first stage of growth aggregates of similar sizes collide very gently at millimeter per second or less. Once objects reach a size of several centimeters the impact energy is sufficiently high to initialize their compaction (Blum and Wurm, 2000). The compact aggregates do not couple to the gas as well as the fluffy aggregates did and relative velocities between the gas and the dust aggregates increase. At the same time the relative velocities become size dependent, increasing with size (Weidenschilling and Cuzzi, 1993; Sekiya and Takeda, 2003). The different velocities relative to the gas directly translate into relative (collision) velocities between different particles and particles of different sizes collide at much higher velocities now. A body (dust aggregate) of 1 m might collide with smaller bodies at velocities of several tens of meter per second (Weidenschilling and Cuzzi, 1993; Sekiya and Takeda, 2003).

So far experiments on small dust aggregates have only resulted in fragmentation at higher speeds (Blum and Wurm, 2000; Blum and Münch, 1993). Related experiments including more solid projectiles or targets like marbles or ice spheres also only showed a transition from sticking to rebound or fragmentation (Kouchi et al., 2002; Supulver et al., 1997; Colwell and Taylor, 1999; Colwell, 2003; Bridges et al., 1996). Therefore, it has been an open question if a mechanism exists by which high speed collisions can lead to net growth of a larger body.

In earlier experiments we showed that the result of a collision which is initially eroding can still lead to net growth if the gas in the protoplanetary disk and its motion relative to the colliding bodies is considered (Wurm et al., 2001a, 2001b). The gas flow in protoplanetary disks can return ejected dust to the eroded body and add mass. Sekiya and Takeda (2003) considered the gas flow in more detail and came to the conclusion that in the inner region of protoplanetary disks (<5 AU) this mechanism of gas aided growth might work for solid (non-porous) bodies of a few meters in size. They conclude that a change in the gas flow regime from free molecular to continuum flow then leads to a transport of ejecta around a body rather than back to its surface. While this is true for a solid non-porous body we showed recently that even in the continuum regime reaccretion of fragments can occur if the eroded body is highly porous (Wurm et al., 2004). Then gas will not only flow around but also through it. Ejecta of a collision which stay entrained in this part of the gas flow entering the body will return to the surface of the eroded parent body and might eventually lead to net growth. The efficiency of this mechanism depends on the porosity and morphology of the body and the sizes and velocities of the ejected particles. The latter would typically need to be below 1 m/s or on the 1% level of the impact velocity for micrometer-sized dust particles assuming the highest collision velocities to be 100 m/s. While 1% seems to be a low value, experiments with solid impactors into a regolith-like target show that these values are reasonable (Colwell, 2003).

It might be expected that even more energy is dissipated if the projectile also consists of dust and if the dust is even finer than in the experiments by Colwell (2003) or if the dust is a larger and more compact agglomerate than in our earlier experiments (Blum and Wurm, 2000). Finally, as shown in this paper, it is important to carry out the experiments at the expected high velocities. The experimental results reported in the literature are thus not applicable to larger bodies consisting of strongly cohesive dust colliding at high velocities. We therefore carried out experiments with millimeter-sized projectiles impacting a centimeter-sized target where both bodies are agglomerates of micrometer-sized dust particles.

In a first set of experiments reported in Wurm et al. (2005), we observed dust impacts into very porous targets and found ejecta which are numerous but very slow as required for gas aided growth. This would be applicable if reaccretion of small dust aggregates leads to a very porous rim of a larger body essentially resulting in a structure which might be described by a ballistic particle cluster growth process (Blum and Schräpler, 2004).

However, this might not be the only scenario for collisions between pre-planetesimals. It cannot be decided yet how the larger bodies really evolve self consistently after many collisions. It is possible that the impacts lead to a more compact body on average. Therefore, a question worth asking is what happens in a collision between a projectile and a target which are both consisting of dust but where the dust sample is packed rather densely. These kinds of experiments are the subject of this paper.

2. Experimental setup

For a dust sample we used a commercial SiO_2 powder with a broad size distribution. Particle sizes are between 0.1 and 10 μm with 80% of the particle mass within particles of 1–5 μm in size. The particles have irregular shapes. The density of the bulk material is 2.6 g/cm^3. A scanning electron microscopy image of the dust can be found in Wurm et al. (2005). The targets were prepared by compressing the dust manually into a target tray. The porosity is $65.7 \pm 1.0\%$, where porosity is defined as void volume over total volume of the dust within the tray. The projectile is compacted in a smaller volume, removed from its mold, and inserted in a holder of similar size for launch. As holders for the projectile we used slightly cone shaped reservoirs consisting of Teflon with an 8-mm diameter opening on the bottom, a 7-mm diameter at the top, and a length of 10 mm. Aluminum foil was used to prevent the dust from falling out while hanging upside down. The aluminum foil is covering most of the opening of the holder but is only fixed (clamped) on one side. It is only 10–20 μm thick. Already the weight of the dust projectile slightly bends the foil elastically. Since the foil is that thin it easily snaps down inelastically at a slightly

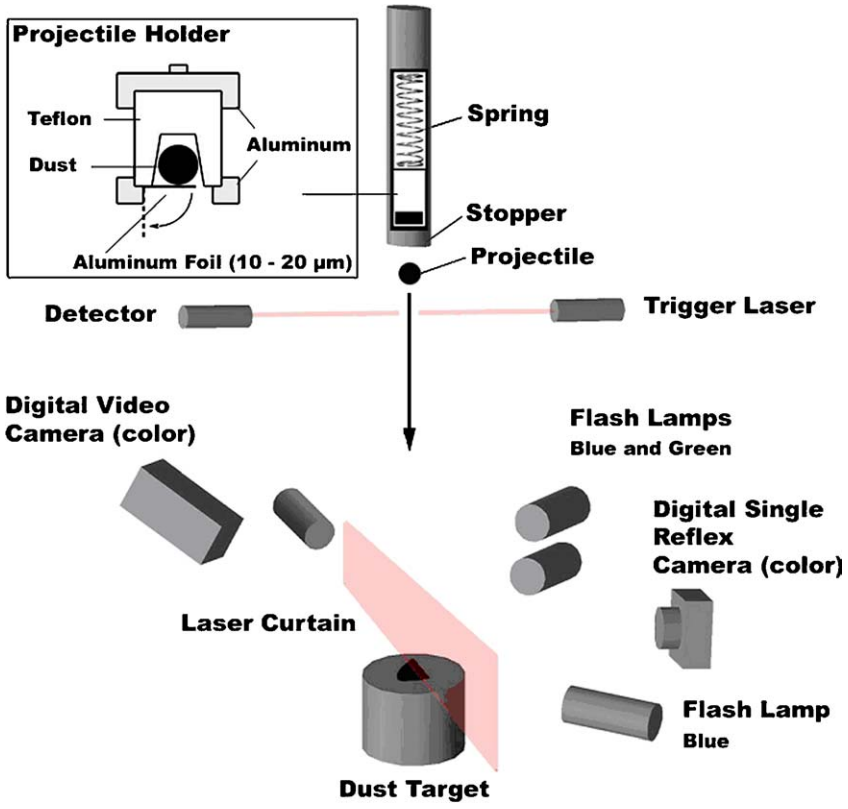

Fig. 1. Sketch of the experiment. A dust projectile is launched onto a dust target after its holder is abruptly stopped. The holder itself is accelerated by a spring. An aluminum foil of only 10–20-µm thickness is fixed on one side of the bottom of the holder. It prevents the dust from falling out while hanging upside down. It essentially covers the whole opening but easily bends inelastically at its fixation point under a load slightly exceeding the weight of the dust projectile. Thus it is easily pushed out of the way by the dust projectile during launch. The load applied to the dust projectile by the foil is insignificant and has no influence on the launched projectile. A light barrier triggers a sequence of flashes in different colors which result in one frame of the single reflex camera containing information of different times before and during the impact. The images are in reflected light. In addition, a laser curtain in the focal plane of the single reflex camera gives information on slower particles in a thin sheet. The aperture of the digital single reflex camera is open for several seconds. The digital video camera is running at a standard frame rate. The dust target is weighed before and after an impact. All experiments are carried out under vacuum.

larger load. After launch by a compressed spring the projectile holder is guided in a tube to about 15 cm above the target where it is instantaneously stopped at the base plate. The base plate has a central opening. Due to inertia the dust within the holder moves on, the aluminum foil bends, and a dust projectile is launched. The effect of the aluminum foil on the fast moving projectile is negligible. It is just pushed out of the way by the projectile. The projectile has an initial porosity comparable to the target porosity of $66 \pm 2.0\%$. Due to the uneven acceleration by the spring and friction while it leaves the holder the projectile might break up. Usually one large dominant fragment is accompanied by a small cloud of smaller fragments as seen in Fig. 2b. Since the extend of the dominant fragment is comparable to the original projectile size we assume that the launch and small degree of fragmentation is not important for the impact. It has to be noted though that the impacts are individual events with slightly different sized and different shaped dust aggregate projectiles of a typical size of 5–10 mm.

The impacts take place in a vacuum chamber (32 cm in diameter) that is evacuated to pressures below 0.01 mbar. Gas drag at these pressures only slightly influences the trajectories for small sub-micrometer-sized particles (fragments). This is of minor importance here. Fragment motions are otherwise determined by gravity. The target is an aluminum tray, 6 cm in diameter and 5 cm deep, filled with dust and centered in the middle of the chamber. A sketch of the setup can be seen in Fig. 1.

In general an individual experiment might be described as follows: A target which has been under predefined low humidity conditions for a few hours is weighed and then placed into the vacuum chamber. The chamber is slowly evacuated to a pressure, p, on the order of $p < 0.01$ mbar. A projectile is launched from above to the center of the target. A few centimeters above the target the projectile passes a light barrier and triggers a sequence of images. Images of the projectile and the impact are recorded by a digital single reflex camera that is directed horizontally to the target surface and is operated in long duration exposure mode so that just one color frame is taken for each impact. However, due to the flash-lamp illumination different images corresponding to different times can be extracted from the different color channels of this one frame. In addition to that a digital video camera with standard video frame rate is used to observe the

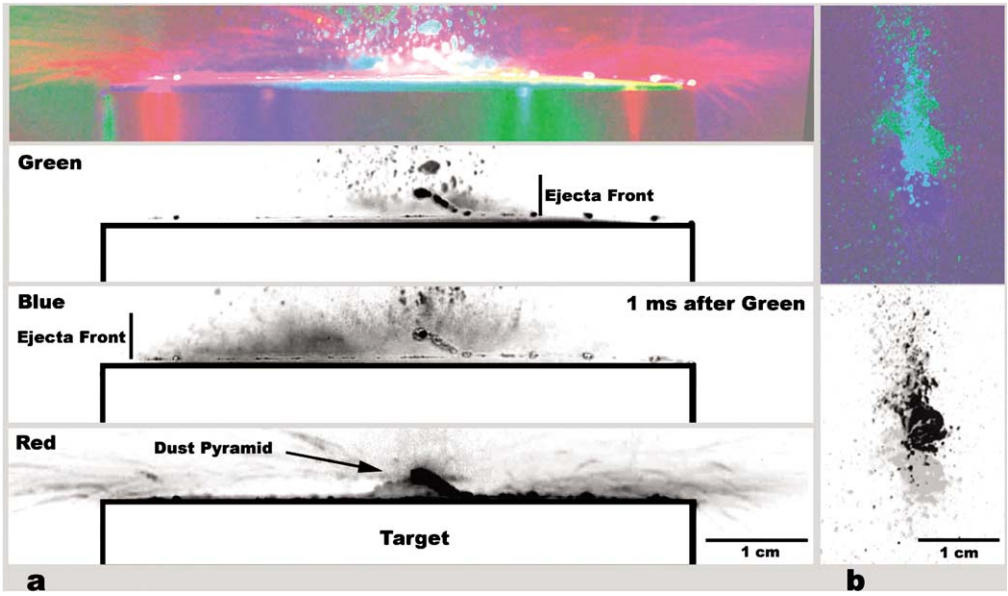

Fig. 2. High velocity impact at 23.7 m/s imaged on one color frame (top). The individual color channels are shown below on a grayscale. Here, the target outlines are marked. The target surface is perpendicular to the image plane. The projectile moved from top to bottom. Therefore, the impact is seen from the side. Two flashes with a time difference of 1 ms in green and blue are fired shortly after the impact. A diffuse dust cloud can be seen spreading to the side. From the ends of this cloud (ejecta front) the maximum ejecta velocities can be estimated to be 9.8 m/s. With particles moving in all directions no restrictions on the lower velocity end of the ejected fragments can be taken from the diffuse cloud. Also visible in red light are slower ejecta illuminated by the laser sheet (see Fig. 1) which is on for the whole time during which the camera aperture is open (4 s). The pyramid-like dust pile that forms due to the impact can be seen in the center of the target and is marked on the red channel. Shown on the right is a projectile as imaged at two different times.

impact from the opposite direction at another viewing angle from above the target.

The flash sequence starts with a green flash-lamp firing once. This results in an image of the incoming projectile in reflected light at a certain distance (∼5 cm) above the target. At a time (usually) $t = 0.5$ ms after the green flash, a blue flash-lamp fires. This results in a second image of the incoming projectile. Due to the color separation the different information can be extracted from a single image of the digital color single reflex camera. The time difference between the flashes and the measured distance on the images give the velocity of the projectile.

These first images also give the size and some information on the shape of the incoming projectile (see right column of Fig. 2). The projectiles in general look rather diffuse. This information has to be used with care though. The video camera using the green flash for bright field illumination reveals that the projectiles are optically thick. Parts of the projectile at the rim can cast shadows seen as dark parts in reflected light. This can mask the true shape of the projectile. However, the overall extent of the observed projectile roughly matches the initial dust projectiles.

The launcher is based on a compressed spring and different modifications have been used for the experiments reported here (different springs, spring compression, projectile holders). Thus, the inner structure of the projectiles might not necessarily be identical throughout all experiments. However, we cannot trace back any of the effects reported in this work to the visual appearance of the projectile. Thus, we do not regard the launch process as a significant parameter here. After imaging of the projectile by two flashes two more flashes in green and blue fire at predetermined times. This gives images of the impact as seen in Fig. 2.

Depending on the exact timing of the flashes the velocity of the fastest fragments can be measured. The dust cloud is usually optically thick and moving in all directions. It can qualitatively be seen that the ejection is very flat with respect to the surface. We will quantify this later in this paper. In addition, a red laser curtain perpendicular to the surface which is sensitive to slower particles has sometimes been used.

After impact the chamber is slowly filled with air again and the target is weighed a second time after spending a few hours under the same low humidity conditions as before the experiment. In addition, for some experiments we sampled the fragments by imaging the inner wall of the chamber and a collector plate which was placed below the target.

3. Slow impacts

Though we just described the procedure for most of the experiments reported here we start with similar experiments which have been carried out in a significantly different manner. In a small number of experiments the projectile was free falling without initial acceleration. In these cases illumination was placed in a way to provide a bright field image in green and red. At a fall height of about 2 m this resulted in impact velocities, v_{imp}, of $v_{\mathrm{imp}} = 6.7$ m/s. The dust was compacted within the projectile holder for these experiments. Therefore, more individual dust particles get

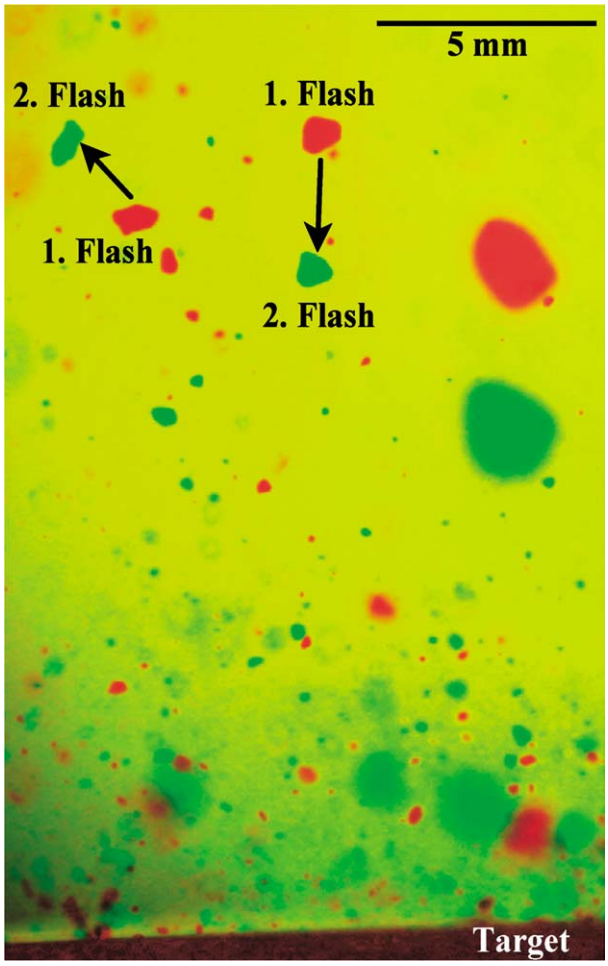

Fig. 3. Contrast and color balance enhanced section of an image with slow velocity impacts (6.7 m/s) of a number of projectiles onto a compact target. Bright field illumination is used with a red and a green flash lamp. The red flash (light gray in black and white image) is triggered later than the green flash (dark gray) so the green particles (light gray) correspond to later times on their trajectories. While impacting particles essentially have to move on straight lines toward the target, ejected particles are heading away from the target in arbitrary directions. Two examples for an impacting (right) and ejected particle (left) are marked.

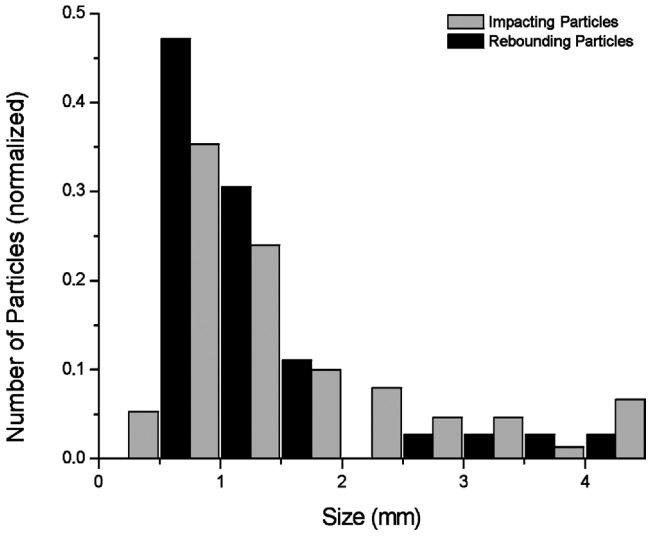

Fig. 4. Size distribution of impacting (gray) and ejected (black) particles normalized to a total sum of 1. A total number of 36 ejected and 150 impacting dust aggregates were measured. Only particles which could clearly be identified twice (imaged at different times) on Fig. 3 (whole image of the section shown) were counted. Ejected particles can move in different directions which produces more ambiguity in matching particles. Impacting particles which have to move down can be matched more easily. Therefore, a smaller total number of particles could be identified as ejected. No ejecta could be identified unambiguously in the smallest size bin. The largest size bin includes all particles larger than 4 mm. The two distributions are similar with a tendency of the ejected particles to be slightly smaller. This implies a small degree of fragmentation during impacts. Ejecta are essentially rebounding projectiles.

in contact with the walls of the holder which increases the friction between projectile dust and holder. Due to this high friction the projectile strongly breaks up during launch. This results in a large number of smaller individual projectiles. Since these projectiles are also slightly dispersed in the horizontal direction they do not interact with each other further on and we get a large number of independent impacts distributed over the whole target surface in a single experiment. An image showing a section of a slow velocity impact is seen in Fig. 3.

We compare these impacts with experiments by Blum and Münch (1993) which had similar (somewhat smaller) impact velocities. In their experiments (among others) individual compact millimeter-sized dust aggregates collided with each other. Our projectiles were also compact millimeter-sized dust aggregates though consisting of different dust samples. With our target being large compared to the projectiles the collisions might be comparable to the case of aggregates with large size difference as measured by Blum and Münch (1993).

Since our experiments usually result in a fragmentation of the projectile we will call the dust leaving the target ejecta. This will include projectiles which only fragment slightly and essentially rebound. On the images (Fig. 3) incoming projectiles and ejected fragments can be seen and distinguished by their headings visualized by two subsequent flashes in different colors. Here, green and red flashes were used for bright field imaging. While we cannot distinguish the individual collisions and ejecta of a given part of the projectile we have a large number of projectiles impacting. One image thus gives an average for many individual collisions. We determined the sizes of the particles on one of the images in more detail. A histogram is shown in Fig. 4.

Ejecta sizes are comparable to the incoming projectile sizes so fragmentation of the projectiles is not very effective. There is a tendency that ejected particles are slightly smaller though. Small fractal aggregates would be completely destroyed at these velocities (Blum and Wurm, 2000). The compact dust aggregates are rather stable. This is probably due to a much larger number of contacts between dust particles which have to be broken to separate parts of the projectile or target. However, the projectiles do not show a large affinity to stick to the target in contrast to the high velocity

impacts reported later. All particles that eventually settle on the target due to gravity can easily be dropped or blown off (under atmospheric pressure) leaving a target surface which looks much the same as before the impacts on a macroscopic scale (for the naked eye). This behavior is used in the high speed impacts to remove fragments from the target which only return to the target due to gravity but do not stick there which marks them as ejecta of the primary collision.

3.1. Ejecta velocity coefficient

An important quantity for an impact is the ejecta velocity coefficient, R, which we define here as

$$R = \frac{v_{\text{eject}}}{v_{\text{imp}}} \tag{1}$$

with v_{eject} being the speed of a particle ejected from the target after a collision, and v_{imp} is the impact velocity of the projectile. We analyzed the velocities of all particles counted in Fig. 4. Fig. 5 shows a histogram of these velocities for the projectiles and the particles ejected.

An average value for the ejecta velocity coefficient is $R = 0.21 \pm 0.08$. This is somewhat smaller than the values found in the work by Blum and Münch (1993). For the case of colliding particles with large size difference they get $R_N = 0.36 \pm 0.03$, where R_N is the coefficient of restitution with respect to the velocity components in the impact direction. Blum and Münch (1993) varied the impact velocity in a range from $v_{\text{imp}} = 0.15 \ldots 4$ m/s and found only 2 cases (out of 24 collisions) of fragmentation at the highest impact velocities. This is comparable to our observation of only a small degree of fragmentation at 6.7 m/s (see Fig. 4). It has to be considered that Blum and Münch (1993) used a different material ($ZrSiO_4$). The individual particle sizes are comparable though to our SiO_2 particles. The lower ejecta velocity coefficient found in our experiments might be due to the difference in particle powder or due to the somewhat higher impact velocities. Overall our results are comparable to their findings.

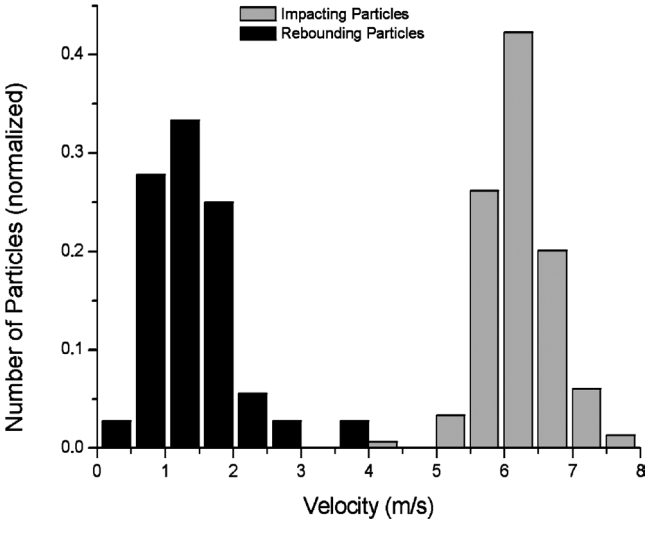

Fig. 5. Velocity distribution of particles for impacting (gray) and ejected (black) particles normalized to a total number of 1 for each distribution. The average velocities are $v_{\text{imp}} = 6.7$ m/s for the impacting particles and $v_{\text{eject}} = 1.4$ m/s for the ejected particles. v_{eject} is the absolute value of the velocity of the fragments in the given direction. The average ejecta velocity coefficient is $R = 0.21 \pm 0.08$.

It should be noted that these results suggest that this kind of slow collision might not be very favorable for growth of a larger object or eventually planetesimals. However, increasing the impact speed yields a completely different picture as seen in the following section.

4. Fast impacts

We conducted a total of 25 experiments with impact velocities up to about 25 m/s. A typical image of a high velocity impact is shown in Fig. 2. Each impact is imaged on one frame with four flashes by the digital single reflex camera. Two more frames before and after the impact give further information about the static conditions of the target before and after the impact. The fastest impacts result in a cloud of fragments. From the outer extent of the dust cloud in different colors corresponding to different times the maximum ejecta velocity is determined to be $40 \pm 10\%$ of the impact velocity which is an ejecta velocity coefficient $R = 0.4 \pm 0.1$ for collisions faster than 20 m/s. Due to the two-dimensional imaging no limit on the smaller fragment velocities can be taken from the clouds. By varying the timing of the flashes we are able to resolve different phases of an impact. If we decrease the time before the 3rd and 4th flash the images reveal what happens during impact. This means that part of the projectile has already been in contact with the target while the upper part is still on its way down to the target. These images reveal that the formation of the dust cloud starts as soon as the first parts of the projectile get in contact with the target. Leaving with 50% of the impact velocity or less only fragments at the outer edges of an impacting projectile can escape immediately. Others are hit by following parts of the projectile. The escape of fragments thus depends on the shape of the projectile (front side) and explains why ejection at certain directions can be enhanced or depleted as seen on the inside walls of the chamber (described below). There is a tendency that the projectile sticking to the target builds a pyramid-like structure with a base comparable in size to the original size of the projectile often leading to a point-like tip.

A number of fragments are found to be only lying on the target after an experiment rather than being rigidly stuck to it. These particles can easily be dropped off just by tilting the target more than 90°. It has to be noted that the original target—though porous—is a strongly cohesive compound of dust particles in our experiments. No dust is removed from the original target if it is tilted 90° or more.

The main part of the projectile makes intimate contact with the target after an impact (i.e., sticks). It cannot be dropped nor brushed off easily but qualitatively shows a sim-

ilar resistance to force as the rest of the target. This fraction of the projectile that is strongly connected to the target must have resulted from the original impact and not from any ejecta returning to the target which would be an artifact of doing the experiment in 1 g. This is because any material falling back to the target after an initial ejection would strike at a much lower speed, comparable to the experiments described in Section 3. Such returning ejecta would not stick rigidly and would easily drop off after tilting the target. Tilting the target after an experiment thus allows to remove any ejecta that was reaccreted due to gravity. Therefore, we do see accretion which must not be attributed to gravity but results from the impact itself. Only very small ejecta with a large (contact) surface to mass ratio are able to rigidly stick to the target after returning due to gravity and to withstand tilting of the target. In fact a few percent of mass is almost always accreted due to this effect as quantified below and seen in Fig. 6. This fraction would not be accreted under microgravity but is small compared to the mass of the main part of the sticking projectile.

We also exclude that slow ejection and reaccretion of a significant amount of material from the original target occurs unnoticed. For dust particles ejected too slow to be noticed the kinetic energy would be comparable to the binding energy of the dust particles (Wurm et al., 2005). Since our original target is highly compact any change in the surface at that level has influence on neighboring parts and would immediately be visible on a larger part of the target, i.e., resulting in larger chips of dust. These parts would also drop off if the target is turned. We did not notice any change on the target surface of this kind.

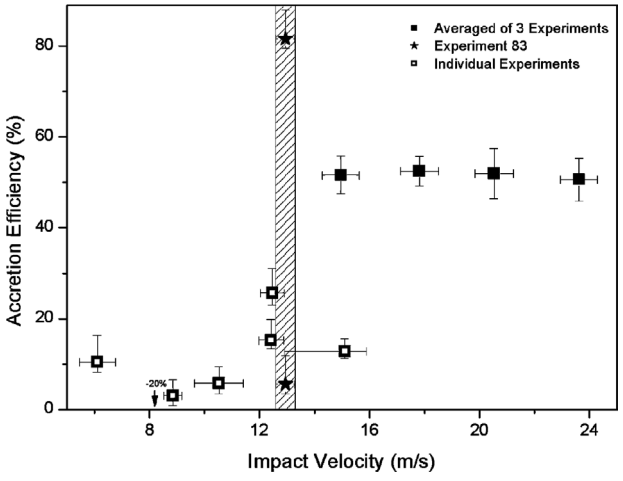

Fig. 6. Accretion efficiency over impact velocity. Accretion efficiency refers to the mass gained by the target with respect to the projectile mass in percent. The target mass is measured after the free particles which are not bound to the surface have been dropped off by tilting the target. These particles in general would not be on the surface in microgravity. They are slow ejecta that return to the surface due to gravity. In the case of experiment 83 the projectile remained stuck after tilting the target but fell off after applying a slight manual impulse to the target. The filled squares are values averaged over three individual experiments each with accretion efficiency larger than 30%. Due to a larger deviation of individual experiments at high velocities and the larger number of high speed impacts this visualizes the whole data best. The open squares are individual experiments at the lower impact velocities with accretion efficiency below 30%. In one case material from the target was sticking to a fragment leaving, which resulted in mass loss of the target of 20%.

The implications of our experiments are rather important. Even if 50% of the smaller body in a collision between two compact dusty bodies would be shattered to very small pieces the remaining part adds mass to the larger body which could therefore grow even in these high speed collisions.

4.1. Accretion efficiency

One of the most important quantities for an impact with respect to the question if planetesimals can form is the mass gain/loss during a collision. The accretion efficiency for the experiments as a function of the impact velocity is shown in Fig. 6. Accretion efficiency is defined here as mass difference of the target after an impact with respect to the projectile mass. An accretion efficiency of 1 (100%) thus means that the whole projectile mass has been added to the target, which would be the maximum achievable.

As mentioned before, at the highest velocities (25 m/s), a large part of the projectile sticks to the target which can be as much as 50% of the projectile mass. This value can vary for an individual collision from about 30 to 70% but on average is constant down to impact velocities of about 13 m/s. As the impact velocity decreases below this threshold only a little mass sticks to the target. This is consistent with the slow collisions described above. The remaining few percent sticking to the target might be very small fragments which would indeed be able to stick to the target at low impact velocities after one or several rebounds. Under microgravity this fraction of sticking dust might be reduced but this has to be studied further. We observed one impact (labeled no 83) just on the edge of sticking. The projectile was essentially intact and stuck to the target; it remained stuck while the target was tilted, but a mild knock loosened it. In another case, some mass from the target was observed to be stuck to an ejected projectile which would lead to a slight mass loss of the target.

The experiments show that the fragments become larger at intermediate and low speeds, approaching the original size of the projectile for the slow velocities, in agreement with the results given above for the free fall experiments. For intermediate speeds large aggregates can be found bouncing off but leaving an imprint into the target surface which can be several millimeters deep. Therefore, the target is not behaving like a solid surface but actively takes part in the impact even if it is compact. How the structure of the target is changed due to the impacts has to be the focus of future studies.

4.2. Wall observations

With ejecta measured to be faster than 9 m/s for the high speed collisions the trajectories within a 32-cm cham-

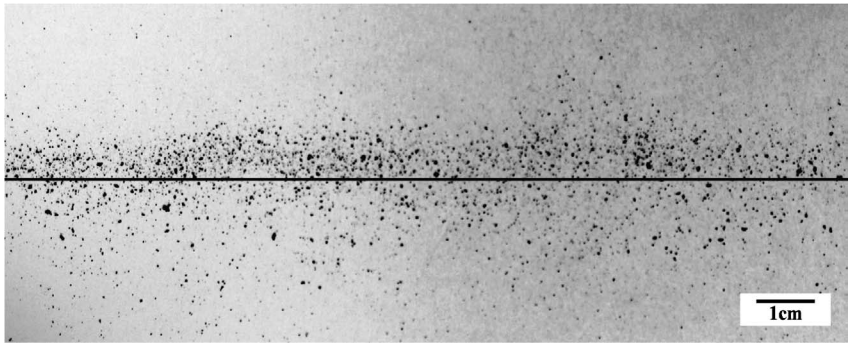

Fig. 7. Image of particles at the inner chamber wall (inverted for visibility here). Marked as solid line is the approximate position of the target plane.

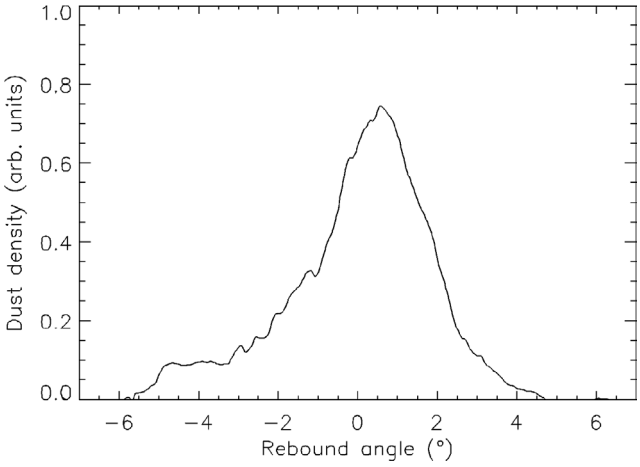

Fig. 8. Distribution of dust particles with height over the plane of impact. The height profile is the sum of intensities (pixel brightness) for a given height averaged over 25 horizontal pixel lines taken from the image in Fig. 7. The height has been transformed to angles with respect to the target surface and through the target center, keeping in mind that the actual headings of fragments might be smaller if they do not lift off at the target surface but rather at the upper parts of the pile created by the projectile. We estimate the systematic error of the angular scale to be 1°.

ber (16 cm from the center to the walls) are almost straight lines. It is interesting to note what happens when the fragments hit the wall of the chamber. An image of particles at the chamber wall can be seen in Fig. 7.

Most of the particles ejected during fast impact stick to the wall. There is a rather sharp line of particles at target height. This implies that the ejection angles with respect to the target surface are rather flat in qualitative agreement with the images of the impacts. To quantify the distribution of particles in height over the plane of impact we summed up the intensity (pixel brightness) for a given height in image Fig. 7. The resulting height profile of fragments is shown in Fig. 8.

Particles are essentially limited in height to 1 cm above the target surface with a strong concentration toward smaller heights. There is a number of particles below the target plane. These particles are probably indeed heading downward with respect to the target plane and originate at locations of the sticking projectile above the target. The lower limit is roughly in agreement with straight trajectories from the top of the sticking projectile to the wall. In detail there is ambiguity if particles on the wall originate, e.g., at the bottom of the projectile (target surface) and move slightly upward or if they move horizontally but originate further upward on the projectile pile. Assuming the majority of fragments originating at the target level a maximum ejection angle can be estimated to be 3° with respect to the target plane. While we marked the plane of the surface by a laser tangential to the upper target end the dust plane is, e.g., never completely flat. We estimate an error of 1° for the angular scale in Fig. 8 which is included in the maximum ejection angle of 3°.

The ejection angle is a very important parameter which might determine the fate of the fragments in protoplanetary disks. Wurm et al. (2004) show that gas flow through a porous body can return fragments after a collision. To be reaccreted by gas flow an ejected particle has to stay close to the surface. If ejection angles are extremely small even high speed fragments stay close to the surface and might be reaccreted. Also on a rough target surface such fragments might hit a bump on the target again at high velocities which leaves more material sticking.

The analysis of the wall fragments assumes that particles hitting the wall are actually sticking there and that no major part is ejected from the walls. However, this is very plausible. No significant amount of dust could be found falling down on a sheet of black paper that was put under the target over the whole chamber cross section. Here, mostly dust is seen that is slowly ejected and falls down close to the target. This slow dust is responsible for numerous parabolas imaged in the laser as seen in Fig. 2. The total dust mass of these slow fragments is small (about 10% or less of the projectile mass) for the high speed impacts and increases in mass for the slow impacts where eventually it makes up all the fragment mass. For the high speed impacts the slow fragment fraction is clearly separated from the fast fraction sticking to the wall and we only consider the high speed fraction here further. The main impacts onto the target suggest that a large amount of dust should stick to a compact target at velocities of 13 m/s or higher. For the high speed collisions the fragments reaching the wall still have high velocities though with 9 m/s the lower limit might be significantly slower. This ac-

tually gives another set of data for high velocity impacts of smaller dust aggregates. We note that the wall is a solid surface rather than consisting of dust. Since the main impacts onto the target show that the target material takes part in the collision the impacts onto the wall are fundamentally different.

Particles sticking to the wall unambiguously show sticking without influence of gravity since the dust would fall down otherwise if it was ejected. From earlier experiments we know that aggregates consisting of irregular micrometer-sized particles and grown in a cluster–cluster aggregation process would not stick to the wall above ∼3 m/s velocity (Blum and Wurm, 2000). The small dust aggregates hitting the wall thus have to be (more) compact and their sticking behavior can be compared to the collisions of the primary large projectiles. In both cases sticking of a large fraction of the projectile at high velocities occurs. Thus, for projectiles in the range from ∼50 μm (see next section about size distribution) to ∼1 cm net growth at collision velocities larger than 9 ± 1 or 13 ± 0.5 m/s, respectively, seems possible. It has to be kept in mind that the impacts onto the wall are onto a solid surface.

4.3. Ejecta size distribution

Most of the mass of an ejected dust aggregate which hits the wall in the high speed collisions sticks there. We could only see a minor amount of dust on the cardboard below. We thus regard it as an appropriate assumption that the sizes of dust aggregates on the wall are closely resembling the sizes of ejecta generated in the main impact. For the small and intermediate impact velocities size distributions are not as straightforward to obtain. However, we measured three size distributions of fragments for three successive experiments carried out at velocities above 20 m/s shown in Fig. 9.

The size distribution has two regimes. For small particles the size distribution is flat and might be described by a constant. For larger particles the size distribution follows a power law with index -5.6 ± 0.2. The transition between both regimes is at about $s = 0.5$ mm in size. There is a cut-off for large particle sizes at about 1 mm for the given impact parameters. Only very few larger fragments are found. As far as the mass is concerned the maximum is at about 550 ± 50 μm. Thus, the mass of a projectile of 1 cm which is redistributed to the dust phase in a protoplanetary disk after a collision could be found in dust aggregates of more than one order of magnitude smaller in size. This also shows that larger dust particles observed in protoplanetary disks are not necessarily just grown but might be debris particles from collisions of bodies which are already much larger.

5. Discussion

It has to be noted that our target size is limited and confined by a solid aluminum tray. If a target of the same size

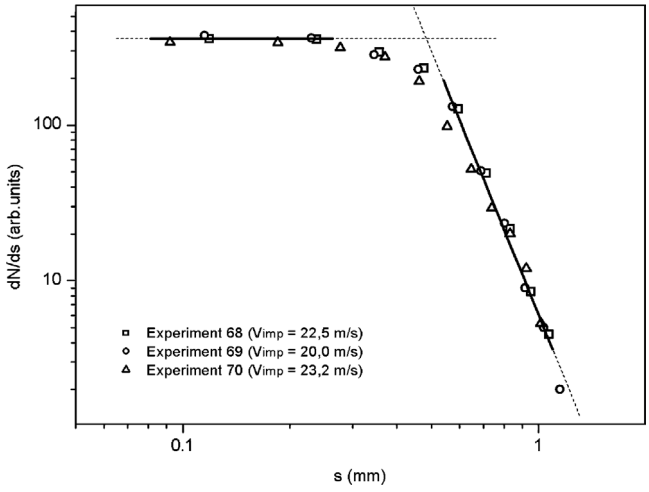

Fig. 9. Size distribution of fragments for three successive experiments at high collision velocities. Shown is the number of particles per size bin ($\mathrm{d}N/\mathrm{d}s$) over the size of the fragments. A total of 989, 1512, and 847 particles were measured for experiments 68, 69, and 70, respectively. For comparison all size distributions were adjusted in height by a factor (manually chosen iterative) as to qualitatively give the best match with each other. All size distributions essentially follow the same functional behavior. For small particles the size distribution is constant. For larger sizes the size distribution follows a power law with power -5.6 ± 0.2. The transition occurs at a size of about $s = 0.5$ mm. There is a sharp cut-off at 1 mm size. Only very few fragments can be found which are (slightly) larger.

(6 cm) were used without supporting tray, effects might be visible which cannot be seen within the tray. Our recent experiments on highly porous targets show a projectile which penetrates into the target dust but is being stopped after about 1 cm (Wurm et al., 2005). A subsequent impact onto the same position compresses the target further by a comparable amount. The other parameters besides the target porosity are similar to the experiments reported here. Thus the projectiles in our experiments would probably not just go straight through the target if the tray was removed. It is possible though that effects like ejection of dust at the backside would be visible. It is also thinkable that still smaller compact targets without tray would be cracked or fragmented. Considering that very compact bodies and the high velocities might only show up in protoplanetary disks for bodies of size much larger than 10 cm (Weidenschilling and Cuzzi, 1993), our supporting tray might be regarded as merely a substitute to simulate the inertial mass of a larger compact body. So far we only see very local effects on the target morphology at the target surface. We thus regard the experiments with compact targets and supporting tray as good analogs for targets of larger sizes. This assumption certainly has to be tested but this requires a different setup and probably microgravity experiments, which is beyond the scope of this paper.

The high speed impacts into targets of different morphology, e.g., for very porous targets (Wurm et al., 2005), and compact targets reported here clearly show that the make-up of the target is one of the major parameters determining the outcome of a collision. The first collisions after compaction

of fluffy dust aggregates are slow and the targets might keep a high porosity after accommodation of the projectile and grow (Wurm et al., 2005). Bodies only reach collision velocities above 10 m/s with smaller bodies once they have grown to several tens of centimeter (Weidenschilling and Cuzzi, 1993). This might naturally explain how compact large targets of the type studied here form in the first place. These impacts are one possible complementary scenario for subsequent collisions of larger bodies in protoplanetary disks after high speed collisions have compacted the aggregates more and more. To summarize, the main results of our experiments are

- A large compact dust aggregate of millimeter- to centimeter-size colliding with a compact dust target between 13 and 25 m/s will partly stick to the target. A fraction of about 50% of the mass is added to the target on average independent of the speed as long as it is above the threshold of 13 ± 0.5 m/s.
- Smaller particles from 50 μm to 1 mm also stick to a large degree to a solid target above 9 ± 1 m/s. Probably much more than 50% of the mass is added and the threshold for sticking is shifted a little bit to smaller velocities, compared to the values for larger aggregates. This might be due to the different physics of impacts onto a solid surface compared to impacts onto a dusty surface.
- A projectile of millimeter- to centimeter-size colliding with a compact target at speeds below 13 ± 0.5 m/s will not stick but be ejected or essentially rebound again.
- Ejecta of a high speed collision of millimeter- to centimeter-size projectiles at 25 m/s typically are one order of magnitude smaller in size. At smaller impact speeds fragments get larger. The ejecta size for high speed collisions follows a flat distribution for small dust aggregates up to 500 μm and a power law with power -5.6 ± 0.2 for larger particles with a cut-off at 1 mm.
- Ejecta of a high speed collision are fast with $40 \pm 10\%$ of the impact velocity or an ejecta velocity coefficient of $R = 0.4 \pm 0.1$. This is much higher than in our low speed collisions or in the low speed collisions by Colwell (2003), where the ejecta speeds are typically below 10% of the impact speed. It is also different from high speed impacts into highly porous targets where ejecta speeds are below 1% of the impact speed (Wurm et al., 2005).
- The fragments from a high speed collision at normal incidence are ejected very flat with respect to the target surface at ejection angles below 3°.

With the assumption that these collisions can occur in protoplanetary disks it might be that even though a rather spectacular shower of fragments is observed to be ejected, a net growth of a more massive body in a high velocity impact can immediately occur. This is the first time that net growth in collisions that fast has been observed and studied for dusty bodies.

5.1. A simple model for the impacts

It seems like aggregates are ejected (not sticking) as long as they are essentially not fragmenting and that projectiles leave some part sticking once they fragment significantly. Obviously the energy dissipation due to fragmentation is needed for the process.

If only a little fragmentation takes place the friction between dust particles in the aggregates is so small that there is mostly elastic compression of the projectile and the target. During ejection the connection between projectile and target will break at the weakest contact area which in most cases will be the newly formed interface between projectile and target.

At higher speeds the projectile parts which get in contact with the target get fragmented and are compressed onto the target. The dust will partly behave like a particle fluid and generate a pressure on neighboring particles. In the vertical direction this pressure will be balanced by the projectile parts still further up proceeding toward the target. In the layer parallel to the target surface dust particles can escape at the edges. For the particles at the front of the projectile this removes an outer ring of dust and later projectile parts can fill this gap. The inner particles cannot escape and the projectile dust will pile-up. This explains the pyramid-like structure. Part of the energy is distributed among the escaping fragments but a large fraction of energy is also dissipated by friction between the inner particles which eventually get slow enough to be assimilated by the target surface. The projectile dust hitting the ground latest has no dust on top and no pressure can be build-up. Here, fragments might leave slowly and in all directions. This explains the fraction of slow fragments. This is certainly a simplification and more detailed calculations are needed to simulate these impacts.

Returning to the application in protoplanetary disks a further comment would be that the fragments that do not stick will feed the dust reservoir of the disk again. Observations of disks a few million years old still show evidence of small dust particles (Beckwith et al., 1990; Haisch et al., 2001). A large number of experiments carried out with dust particles in the last decade or so show that collisions between dust particles will lead to sticking at least until centimeter-sized aggregates have grown (Wurm and Blum, 1998; Blum and Wurm, 2000; Blum et al., 2000; Poppe et al., 2000). This has sometimes been assumed to be a contradiction to the observations. However, the later collisions will feed the dust reservoir again as seen, e.g., in this paper, which can easily explain the existence of dust particles even after a few million years. It would, e.g., be possible that half of the mass of solids evolves to planetesimals but the other half stays recycled as dust. This would be a change which would hardly be noticeable in observations. This is just an example though and modeling has to be done to provide the right size distributions during the evolution of the disk, i.e., the solids.

The size distribution of solids will strongly depend on the impacts. This will determine the overall growth as part of an ongoing collisional evolution. Details about collisions at different target porosities and for different morphological parameters are needed to be able to model this evolution self consistently. This paper is one step more to provide the necessary parameters for modeling.

There are still numerous parameters which can be changed and which will influence the outcome of a collision. The experiments leave little doubt though that net growth of a larger body even in high speed collisions can occur. If planetesimals do not form any other way more quickly their formation by collisional growth is very likely.

Acknowledgments

We appreciate that this work is funded by the Deutsche Forschungsgemeinschaft. We thank Josh Colwell and an anonymous reviewer for detailed, very constructive, and helpful comments. Our sincere thanks also go to Raimund Thewes for numerous technical discussions about the set-up and its implementation.

References

Beckwith, S.V.W., Sargent, A.I., Chini, R.S., Güsten, R., 1990. A survey for circumstellar disks around young stellar objects. Astron. J. 99, 924–945.

Beckwith, S.V.W., Henning, T., Nakagawa, Y., 2000. Dust properties and assembly of large particles in protoplanetary disks. In: Mannings, V., Boss, A.P., Russell, S.S. (Eds.), Protostars and Planets IV. Univ. of Arizona Press, Tucson, pp. 533–558.

Blum, J., Münch, M., 1993. Experimental investigations on aggregate–aggregate collisions in the early solar nebula. Icarus 106, 151–167.

Blum, J., Wurm, G., 2000. Experiments on sticking, restructuring, and fragmentation of preplanetary dust aggregates. Icarus 143, 138–146.

Blum, J., Schräpler, R., 2004. Structure and mechanical properties of high-porosity macroscopic agglomerates formed by random ballistic deposition. Phys. Rev. Lett. 93, 115503-1–115503-4.

Blum, J., 26 colleagues, 2000. Growth and form of planetary seedlings: Results from a microgravity aggregation experiment. Phys. Rev. Lett. 85, 2426–2429.

Bridges, F.G., Supulver, K.D., Lin, D.N.C., Knight, R., Zafra, M., 1996. Energy loss and sticking mechanisms in particle aggregation in planetesimal formation. Icarus 123, 422–435.

Colwell, J.E., 2003. Low velocity impacts into dust: Results from the COLLIDE-2 microgravity experiment. Icarus 164, 188–196.

Colwell, J.E., Taylor, M., 1999. Low velocity microgravity impact experiments into simulated regolith. Icarus 138, 241–248.

Dominik, C., Tielens, A.G.G.M., 1997. The physics of dust coagulation and the structure of dust aggregates in space. Astrophys. J. 480, 647–673.

Garaud, P., Lin, D.N.C., 2004. On the evolution and stability of a protoplanetary disk dust layer. Astrophys. J. 608, 1050–1075.

Goldreich, P., Ward, W.R., 1973. The formation of planetesimals. Astrophys. J. 183, 1051–1062.

Haisch, K.E., Lada, E.A., Lada, C.J., 2001. Disk frequencies and lifetimes in young clusters. Astrophys. J. 553, L153–L156.

Kempf, S., Pfalzner, S., Henning, T., 1999. N-particle-simulations of dust growth. I. Growth driven by Brownian motion. Icarus 141, 388–398.

Klahr, H.H., Bodenheimer, P., 2003. A three phase model for planet formation—The formation of a planet in the eye of a hurricane. In: Fridlund, M., Henning, T. (Eds.), Proceedings of the Conference on Towards Other Earths: DARWIN/TPF and the Search for Extrasolar Terrestrial Planets. In: ESA SP, vol. 539. ESA, Noordwijk, pp. 481–483.

Kokubo, E., Ida, S., 2002. Formation of protoplanet systems and diversity of planetary systems. Astrophys. J. 581, 666–680.

Kouchi, A., Kudo, T., Nakano, H., Arakawa, M., Watanabe, N., Sirono, S., Higa, M., Maeno, N., 2002. Rapid growth of asteroids owing to very sticky interstellar organic grains. Astrophys. J. 566, L121–L124.

Poppe, T., Blum, J., Henning, T., 2000. Analogous experiments on the stickiness of micron-sized preplanetary dust. Astrophys. J. 533, 454–471.

Sekiya, M., Takeda, H., 2003. Were planetesimals formed by dust accretion in the solar nebula. Earth Planets Space 55, 263–269.

Supulver, K.D., Bridges, F.G., Tiscareno, S., Lievore, J., Lin, D.N.C., 1997. The sticking properties of water frost produced under various ambient conditions. Icarus 129, 539–554.

Weidenschilling, S.J., 1997. The origin of comets in the solar nebula. Icarus 127, 290–306.

Weidenschilling, S.J., Donn, B., Meakin, P., 1989. The physics of planetesimal formation. In: Weaver, H.A., Danly, L. (Eds.), The Formation and Evolution of Planetary Systems. Cambridge Univ. Press, Cambridge, pp. 131–146.

Weidenschilling, S., Cuzzi, J.N., 1993. Formation of planetesimals in the solar nebula. In: Levy, E.H., Lunine, J.I. (Eds.), Protostars and Planets III. Univ. of Arizona Press, Tucson, pp. 1031–1060.

Wetherill, G.W., Stewart, G.R., 1989. Accumulation of a swarm of small planetesimals. Icarus 77, 330–357.

Wurm, G., Blum, J., 1998. Experiments on preplanetary dust aggregation. Icarus 132, 125–136.

Wurm, G., Blum, J., Colwell, J.E., 2001a. A new mechanism relevant to the formation of planetesimals in the solar nebula. Icarus 151, 318–321.

Wurm, G., Blum, J., Colwell, J.E., 2001b. Aerodynamical sticking of dust aggregates. Phys. Rev. E 64, 046301-1–046301-9.

Wurm, G., Paraskov, G., Krauß, O., 2004. On the importance of gas flow through porous bodies for the formation of planetesimals. Astrophys. J. 606, 983–987.

Wurm, G., Paraskov, G., Krauß, O., 2005. Ejection of dust granules by elastic waves in collisions between mm- and cm-sized dust aggregates at 16.5 to 37.5 m/s impact velocity. Phys. Rev. E 71, 021304-1–021304-10.

Yamoto, F., Sekiya, M., 2004. The gravitational instability in the dust layer of a protoplanetary disk: Axisymmetric solutions for non-uniform dust density distributions in the direction vertical to the midplane. Icarus 170, 180–192.

Youdin, A.N., Shu, F.H., 2002. Planetesimal formation by gravitational instability. Astrophys. J. 580, 494–505.